NASA TECHNICAL MEMORANDUM

NASA TM X-67825

NASA TM X-67825

LOW-SPEED JET NOISE FROM A 1.83-METER (6-FT) FAN FOR TURBOFAN ENGINES

by Gene L. Minner and Charles E. Feiler
Lewis Research Center
Cleveland, Ohio

TECHNICAL PAPER proposed for presentation at Fourth Fluid and Plasma Dynamics Conference sponsored by the American Institute of Aeronautics and Astronautics
Palo Alto, California, June 21-23, 1971

LOW-SPEED JET NOISE FROM A 1.83-METER (6-FT) FAN FOR TURBOFAN ENGINES

Gene L. Minner and Charles E. Feiler
National Aeronautics and Space Administration
Lewis Research Center
Cleveland, Ohio

E-6124

Abstract

The jet noise contribution to the far-field sound from a 1.83-meter- (6-ft-) diameter fan has been determined for two simulated nacelle configurations. One nacelle had hard walls, while the other had acoustic liners on the wall and on inlet splitter rings. The jet velocities, typical of high-bypass-ratio fan engines, varied from 137 to 223 meters per second (450 to 730 ft/sec). The results of the study show that the acoustic liners effectively eliminate low-frequency noise from internal sources. Data from the lined configurations were found to be in good agreement with the eighth-power dependence on jet velocity. Data from the hard-wall configurations, because of the influence of internally generated noise, show higher noise levels and a weaker velocity dependence. The data are also about 6 decibels less than predicted by extrapolation of the SAE curve to the velocities present. This result may be due to the contribution of jet density in the SAE correlation, where jet density appears to the second power. The data were in better agreement with a correlation obtained for unheated jets. The shape of the measured spectra agreed well with the spectra published by the SAE when annulus height of the nozzle was used as the characteristic dimension in the Strouhal number. The directivity of the jet noise was examined and was found to be in good agreement with published results.

Introduction

For high-bypass-ratio fan engines operating at subsonic fan exhaust velocities, there has been considerable interest in the level of jet noise and its dependence on velocity. Theoretical studies of jet noise show that it should follow an eighth-power dependence on velocity (e.g., Refs. 1 and 2). This result is supported by experimental studies at high velocities in general and also at low velocities with simple nozzles where the flows are relatively free from upstream turbulence and flow noise (Refs. 1 and 3); however, engine data at low velocities generally show higher noise levels and a weaker velocity dependence than these nozzle experiments (Refs. 3 and 4). This behavior has been attributed to the emergence of other noise sources at low exhaust velocities (Ref. 5). There it was shown that increasing the turbulence level of the flow through a nozzle results in a significant increase in the noise, coupled with a decrease in its velocity dependence from eighth power to sixth or even fourth power. Since noise floors for an engine are generally assumed to be set by the jet noise level, it becomes important to know how to estimate the jet noise. This is especially true when one considers the weight and size penalities associated with engines designed for low exhaust velocities.

In the present report, far-field sound data from a 1.83-meter-diameter (6-ft-) diameter fan have been analyzed for jet noise content for two nacelle configurations. One of the nacelles had hard walls, while the other had acoustic liners on the walls and on inlet splitter rings. The exhaust velocity of the fan jet was varied from 137 to 223 meters per second (450 to 730 ft/sec). The experimental results are presented in several forms and are compared with correlations from the literature. The fan design details may be found in Ref. 6, while complete acoustic and aerodynamic data are given in Refs. 7 and 8 for the hard-wall and acoustically lined nacelle configurations, respectively.

Symbols

A	nozzle area, m^2; ft^2
c_o	atmospheric speed of sound, m/sec; ft/sec
$OASPL_m$	maximum sideline overall sound pressure level (referenced to 2×10^{-5} N/m^2), dB
$OASPL_{m,p}$	maximum polar overall sound pressure level (referenced to 2×10^{-5} N/m^2), dB
P	sound power, W
R	radial distance, m; ft
T_{isa}	international standard atmospheric temperature, ^oK; ^oR
T_o	atmospheric temperature, ^oK; ^oR
V	velocity, m/sec; ft/sec
ρ	jet density, kg/m^3; lb/ft^3
ρ_{isa}	international standard atmospheric density, kg/m^3; lb/ft^3
ρ_o	atmospheric density, kg/m^3; lb/ft^3

Apparatus and Procedure

The data used here were obtained during testing of a full-scale fan at the Lewis Research Center. The design of the fan and facility are described in Ref. 6. The fan tests included both hard-wall nacelles and nacelle configurations with inlet and exhaust ducts that had been acoustically treated to absorb a portion of the internally generated noise. These two nacelle treatments, hard and lined, and the corresponding data are described in Refs. 7 and 8, respectively. Two nozzle areas were also tested. A summary of the nacelle and nozzle arrangements is given in table 1. The test facility consisted of the fan with a 1.83-meter- (6-ft-) diameter inlet duct mounted in a simulated engine cowl on a concrete pedestal. The fan centerline was 5.79 meters (19 ft) above ground level. The fan nozzle had an annular cross section with a conical centerbody extending approximately 1.52 meters

(60 in.) beyond the end of the outer wall as shown in Fig. 1. The design area of the nozzle was 1.26 square meters (13.56 ft^2).

The acoustic liners (configurations 10 to 13, table 1) consisted of aluminum honeycomb panels faced with perforated aluminum sheets. The inlet liners were placed on the outer wall and on both sides of three splitter rings. Figure 1 shows this geometry and the liner parameters. As shown in table 1, two inlet lengths were tested to vary the length of acoustic treatment. In the exhaust duct, the centerbody and outer wall were lined.

For each nacelle configuration aerodynamic and far-field acoustic data were taken in 5-percent speed increments between 60 and 90 percent of the sea-level standard-day fan design speed. The standard-day conditions were 282.2 K (518.7° R), 1.013×10^5 newtons per square meter (2116.2 lb/ft^2), and 70 percent relative humidity. At each speed, three independent data samples were taken and subsequently averaged.

Aerodynamic data consisted of rake measurements of total temperature, total pressure, and static pressure. These data were used to compute velocity and density profiles in the nozzle exit plane. Acoustic data consisted of microphone measurements of sound pressure level at 10° intervals in the horizontal plane through the fan axis. The microphone locations are shown in Fig. 2. The microphone outputs were analyzed with standard 1/3-octave band filters with center frequencies from 50 to 10^4 hertz. Sound pressure levels were also "corrected" to the standard-day conditions. The random error in sound pressure level was estimated in Ref. 7 to be 1.7 decibels.

Analysis of Data

Aerodynamic Data

Typical velocity profiles in the nozzle exit plane are shown in Fig. 3(a) for the hard-wall configuration. Similar profiles are shown in Fig. 3(b) for a lined configuration. From these figures it is evident that the profiles for the two cases are similar and that the peak velocities are within 8 percent of the mass-averaged velocities obtained by integration over the annulus area. The mass-averaged values were used in correlating the jet noise.

Determiation of Jet Noise

The far-field sound measured by the microphones comes from inside the fan nacelle and from the jet mixing region. Examination of typical sound pressure level spectral and directivity distributions gave the basis for separation of the jet noise from the total measured sound.

As indicated by the SAE curve correlating jet noise spectra (Ref. 9), the maximum sound pressure level due to jet noise should occur at about 100 hertz for jets of the size and speed of the present case. By contrast, the internally generated noise associated with the fan occurs predominantly at higher frequencies in the range of the blade passing tone. For the present fan, this frequency varies from about 2000 to 3000 hertz depending on the fan speed. Figure 4 shows typical sound pressure spectra for several fan speeds at an angular microphone position of 160°. The two sound level maxima decribed can be seen, separated by a relative minimum. The location of the minimum varies somewhat with fan speed; however, it generally occurs at 1000 hertz. Therefore, the noise below 1000 hertz was attributed to the jet, and that above was attributed to sources inside the fan nacelle. For noise following the SAE spectrum mentioned earlier, the contribution of the sound pressures outside of ±3 octaves from the peak value to the overall sound pressure level is less than 1/2 decibel. The selected upper frequency of 1000 hertz is more than 3 octaves above the peak and therefore should include nearly all the jet noise.

Although the jet noise radiates in all directions, a dominant portion of its power radiates through a limited range of angles. In order to determine this range, polar distributions of the sound pressure at the frequency associated with the peak value of jet noise were examined on a 30.5-meter (100-ft) radius. These data are shown in Fig. 5, where the sound pressure level at 100 hertz is plotted against angular position for both hard and lined configurations. The curves are characterized by high levels at large angles and by relative minima at approximately 70°. Thus total sound power for the jet was calculated over the angular positions from 70° to 160°. Because of the much higher sound pressure levels at larger angles, the precise selection of 70° did not have a critical effect on the calculated value of jet sound power. The noise from 0° to 70° is associated with the inlet.

Results and Discussion

The criteria used to separate jet noise from the total noise measured were described in the previous section. In this section the results are presented and compared with other results from the literature. The data of sound power are presented first, followed by a comparison of the measured spectra given by the SAE. Peak values of overall sound pressure level are presented and compared with correlations from the literature, and finally typical directivity patterns are presented and compared with results from the literature.

Correlation of Jet Sound Power

Jet sound power in watts is shown as a function of the Lighthill parameter $\rho_o A V^8 / c_o^5$, also in watts, in Fig. 6. Data from both hard and lined configurations are shown. It is evident that there are two distinct patterns of behavior displayed by the two sets of data. A least squares fit of the data from the lined configurations gave

$$P = 2.3 \times 10^{-5} \left(\frac{\rho_o A V^8}{c_o^5} \right)^{1.0} \qquad (1)$$

The values of ρ_o and c_o are given in table 2. The data from the lined configurations thus correlate well with the Lighthill parameter. The coefficient in Eq. (1) is given in Fig. 15 of Ref. 1 as 5×10^{-5} and in Ref. 2 as 3×10^{-5}.

As previously noted the fan nozzle had an annular cross section with a conical center body.

Noise results from this type of nozzle may not be directly comparable with those from circular nozzles. This difference may account, in part, for the deviation of the measured coefficient from the literature values. Additional work is required to determine geometry effects on noise generation.

The data from the hard-wall configurations, in contrast, lie above the lined configuration data and have a weaker dependence on the Lighthill parameter. A possible explanation for this result is that there is low-frequency noise generated within the fan nacelle and that this noise is effectively removed by the acoustic liners. The possibility that low-velocity jet noise may be dominated by internally generated noise has been suggested previously, for example, in Refs. 3 and 5. In Ref. 5, it is shown that the velocity dependence of the internal noise sources is less than the usual eighth-power dependence found for free jets. Thus, as the velocity is decreased, other sources having a lower velocity dependence become more important contributors to the sound power. This effect could cause the larger sound power and weaker velocity dependence observed for the hard-wall data.

Correlation of Jet Noise Spectra

In Fig. 7, experimental octave spectra are compared with spectra predicted by the SAE correlation of Ref. 9. Data are shown from a microphone at the 150° position for a lined nacelle for several fan speeds. The SAE correlation is based on a dimensionless Strouhal number. In converting the Strouhal number to frequency, use of the annulus height of the fan exhaust nozzle, rather than the SAE-recommended equivalent diameter, gave improved agreement between the measured and predicted spectra and suggests that annulus height is the better of the two choices for the present data. The level of each predicted spectrum was determined such that its overall sound pressure level was equal to that of the measured spectrum. As shown in the figure, the shapes of the predicted and measured spectra agree reasonably well. The largest differences occur at the higher frequencies and at the lower fan speeds. This is probably due to the increasing influence of the fan-dominated portion of the spectrum that does not decrease as rapidly with decreasing fan speed as does the jet noise.

Correlation of Maximum Overall Sound Pressure Levels of Jet Noise

The maximum values of overall sound pressure level, $OASPL_m$, have been computed both on a 30.5-meter (100 ft) sideline and on a 30.5-meter (100-ft) radius. In general, the angular position at which the sideline maximum was observed was 130° to 140° from the fan inlet. The polar maximum was obseved at 150° and 160° for the hard and lined configurations, respectively.

In Fig. 8, the sideline data from both hard and lined configurations are plotted in terms of the SAE correlation parameter $OASPL_m - 10 \log (\rho^2 A)$ as a function of jet velocity. The values of ρ are given in table 2. For purposes of the correlation, densities were used in units of lb/ft^3 and areas were used in ft^2. As was true of the sound power data, the hard-wall results are above the lined-wall results and have a weaker velocity dependence. The same explanation applies here also, namely, that the external effects of internal noise, present in the hard-wall configurations, are removed when the acoustic liners are installed. A least squares curve is shown through the lined configuration data. The velocity exponent found for this curve fit was 8.3.

The SAE correlation curve does not extend to velocities less than 305 meters per second (1000 ft/sec). The curve shown in Fig. 8 and attributed to the SAE was obtained by linear extrapolation of the SAE curve on the log plot, using the trend established in the 305 to 610 meters per second (1000 to 2000 ft/sec) range. As shown in the figure, essentially all of the present data lie below the extrapolated SAE curve. The curve describing the present lined configuration data is approximately 7 decibels below the SAE curve. This difference is probably related to the density function appearing in the SAE correlation and perhaps to differences in the mixing zones of annular and circular exhausts. Other investigators have found a weaker dependence of $OASPL_m$ on jet density than the squared dependence given by the SAE correlation. In Refs. 3 and 10, for example, the first-power dependence was found, while in Ref. 11, the total radiated power was found to be independent of jet density.

A typical jet engine exhaust density (such as for the JT3-C, which is one of the engines in the SAE test) is $\rho = 0.423\ kg/m^3$ ($0.0264\ lb/ft^3$). The cold fan jet density was approximately $1.22\ kg/m^3$ ($0.0765\ lb/ft^3$). With a density exponent of zero, there would be a 9 dB shift in the relative positions of the SAE curve and the present data, yielding a difference of approximately 2 dB between them; and of course an exponent of two would leave the 7 dB difference already noted. Additional work is needed in order to ascertain the influence of jet density on noise generation.

A correlation similar to that of the SAE is given in Ref. 2 for both engine data and cold model jets. The correlation parameter, based on the maximum polar value of overall sound pressure level, is $OASPL_{m,p} - 10 \log (\rho_o \rho T^2 A)/(\rho_{isa}^2 T_{isa}^2 R^2)$. In Fig. 9 data from the hard and lined configurations are plotted in this form as a function of jet velocity. From the figure, it can be seen that the data from the lined configurations are in good agreement with curve A. Curve A was obtained in Ref. 3 from nozzle experiments in which considerable effort was expended to eliminate upstream turbulence and flow noise. Data from the hard-wall configurations are somewhat above curve B from Ref. 3. Curve B was obtained from tests of a simulated engine-nozzle rig in which the combustor cans were removed from the upstream piping. The flow in this case was relatively "clean" or free of upstream turbulence or flow noise. From these comparisons it appears that the flow from the present fan nozzle is relatively "clean," even in the hard-wall configuration of the nacelle.

Finally, Fig. 9 also shows curve C from Ref. 3. This curve represents data from a variety of engine and model rig tests. If these data include the contribution of noise from internal sources, it appears that acoustic liners might

offer the possibility of attenuating this noise with the result that curve C could be moved toward curve A or B.

Directivity of Noise

Some representative polar jet noise directivity patterns at a 30.5 m (100 ft) radius are presented in Figs. 10(a) and (b) for lined and hard nacelle configurations respectively. The normalization of the OASPL to directivity index collapses the data to a scatter band around a single curve. However, Ref. 12 shows that Mach number and jet temperature, if varied over a wide range, would have a significant effect on jet noise directivity. The present lined nacelle directivity results are in good agreement with those of Ref. 12 for simple cold jets at Mach numbers of 0.6 to 0.7, also shown in Fig. 10(a). The present hard wall configuration results between 10^{o} and 50^{o} are dominated by fan noise, and have been omitted. There are additionally some minor differences between the hard wall and lined wall results which are unexplained.

The directional patterns of jet OASPL on a 30.5 m (100 ft) sideline are presented in Fig. 11 for configuration 13. The peak values of these curves occur near 130^{o}. The slight drop-off at larger angles is a distance effect, and the rapid drop-off forward of 80^{o} is the result of the greater distance and lower directivity index.

In summary the jet noise directivity results are about as expected, with the peak directivity index occuring at 160^{o} and a peak sideline OASPL near 130^{o}.

Summary of Results

The contribution of jet noise to the total far-field noise from a full-scale fan model has been determined for two simulated fan nacelles. These were a hard-wall nacelle and one in which acoustic liners were placed on the walls and on inlet splitter rings. The data were obtained at the low velocities, 137 to 223 meters per second (450 to 730 ft/sec), typical of high-bypass-ratio fan engines. The results may be summarized as follows:

1. The acoustic liners effectively removed noise from internal sources so that the lined configuration data, either as sound power or as maximum overall sound pressure level, followed the classical eighth-power dependence on velocity.

2. Similar data from the hard-wall configurations had higher noise levels and displayed a weaker velocity dependence than did the data from lined configurations. This was due to a low-frequency contribution to the sound from sources inside the fan nacelle.

3. The overall sound pressure levels from the lined configurations were in good agreement with a correlation for unheated jets, but about 7 decibels less than would be predicted by extrapolation of the SAE correlation for hot jets. It was observed that the discrepancy was probably related to the jet density exponent of 2 used in the SAE correlation.

4. The shape of the sound pressure spectra agreed well with the correlation given by the SAE when annulus height of the nozzle was used as the characteristic dimension in the Strouhal number.

5. The directivity patterns showed low noise levels in the upstream direction and high levels in the downstream direction, with maxima at approximately 130^{o} and 160^{o} for 30.5 m (100 ft) radius and sideline results respectively.

References

1. Lighthill, M. J., "Jet Noise," AIAA Journal, Vol. 1, No. 7, July 1963, pp. 1507-1517.

2. Howes, W. L., "Similarity of Far Noise Fields of Jets," TR R-52, 1959, NASA Cleveland, Ohio.

3. Bushell, K. W., "A Survey of Low Velocity and Coaxial Jet Noise with Application to Prediction," Symposium on Aerodynamic Noise, Royal Aeronautical Society and British Acoustical Society, 1970, paper B.3.1.

4. Lewis, J. H., "Quiet Engine Definition Program. Vol. II. Task I," Rep. PWA-3516, vol. 2, NASA CR-72457, vol. 2, Oct. 1968, Pratt & Whitney Aircraft, East Hartford, Conn.

5. Ffowcs-Williams, J. E. and Gordon, C. G., "Noise of Highly Turbulent Jets at Low Exhaust Speeds," AIAA Journal, Vol. 3, No. 4, Apr. 1965, pp. 791-793.

6. Leonard, B. R., Schmiedlin, R. F., Stakolich, E. G., and Newmann, H. E., "Acoustic and Aerodynamic Performance of a 6-Foot-Diameter Fan for Turbofan Engines. I - Design of Facility and QF-1 Fan," TN D-5877, 1970, NASA, Cleveland, Ohio.

7. Goldstein, A. W., Lucas, J. G., and Balombin, J. R., "Acoustic and Aerodynamic Performance of a 6-Foot-Diameter Fan for Turbofan Engines. II - Performance of QF-1 Fan in Nacelle Without Acoustic Suppression," TN D-6080, 1970, NASA, Cleveland, Ohio.

8. Rice, E. J., Feiler, C. E., and Acker, L. W., "Acoustic and Aerodynamic Performance of a 6-Foot-Diameter Fan for Turbofan Engines. III - Performance of the Noise Suppressors," TN D-6178, 1971, NASA, Cleveland, Ohio.

9. Anon., "Jet Noise Prediction," AIR-876, July 1965, SAE, New York, N.Y.

10. Plumblee, H. E., "Effect of Duct Heating on Jet and Fan Noise," Basic Aerodynamic Noise Research, SP-207, 1969, NASA, Washington, D.C., pp. 113-136.

11. Rollin, V. G., "Effect of Temperature on Jet-Noise Generation," TN 4217, 1958, NACA, Cleveland, Ohio.

12. Grande, E., "Acoustic Scaling Between Model Cold Flow and Hot Flow Jets," D6-20601 TN, 1967, Boeing Co., Renton, Wash.

Configuration		Inlet length	Nozzle area, percent design
Hard	Lined		
1	13	Short (1.524 m; 60 in.)	110
2	10	Short	97
3	11	Long (2.54 m; 100 in.)	97
4	12	Long	110

TABLE 1. - NACELLE CONFIGURATION

Configuration Percent speed	1	2	3	4	10	11	12	13
Jet density, kg/m^3								
60	1.267	1.245	1.260	1.224	1.174	1.209	1.210	1.174
65	1.269	1.241	1.256	1.210	1.171	1.206	1.211	1.171
70	1.266	1.240	1.254	1.219	1.168	1.203	1.211	1.169
75	1.264	1.237	1.253	1.202	1.165	1.200	1.205	1.166
80	1.259	1.232	1.253	1.197	1.163	1.198	1.206	1.165
85	1.254	1.229	1.251	1.262	1.160	1.195	1.200	1.163
90	1.243	1.226	1.251	1.269	1.158	1.193	1.198	1.158
Atmospheric density, kg/m^3								
All	1.283	1.260	1.264	1.244	1.182	1.222	1.231	1.190
Atmospheric speed of sound, m/sec								
All	328	330	331	332	342	336	335	340

TABLE 2. - JET AND ATMOSPHERIC DENSITIES
AND ATMOSPHERIC SPEED OF SOUND

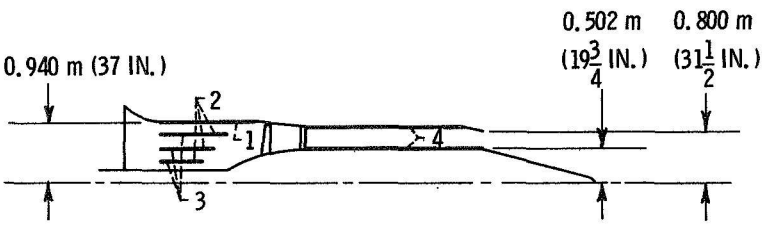

ACOUSTIC LINER CHARACTERISTICS

SURFACE	OPEN AREA RATIO, PERCENT	HOLE DIAMETER		BACKING DEPTH	
		in.	cm	in.	cm
1	2.5	0.032	0.082	0.88	2.24
2	2.5	.032	.082	.20	.51
3	2.5	.032	.082	.68	1.73
4	8.0	.050	.127	.88	2.24

Figure 1. - Cross-sectional sketch of acoustically treated inlet and exhaust ducts for large-scale fan. Plate thickness, 0.051 centimeter (0.020 in.); 0.953-centimeter (3/8-in.) hexagonal honeycomb.

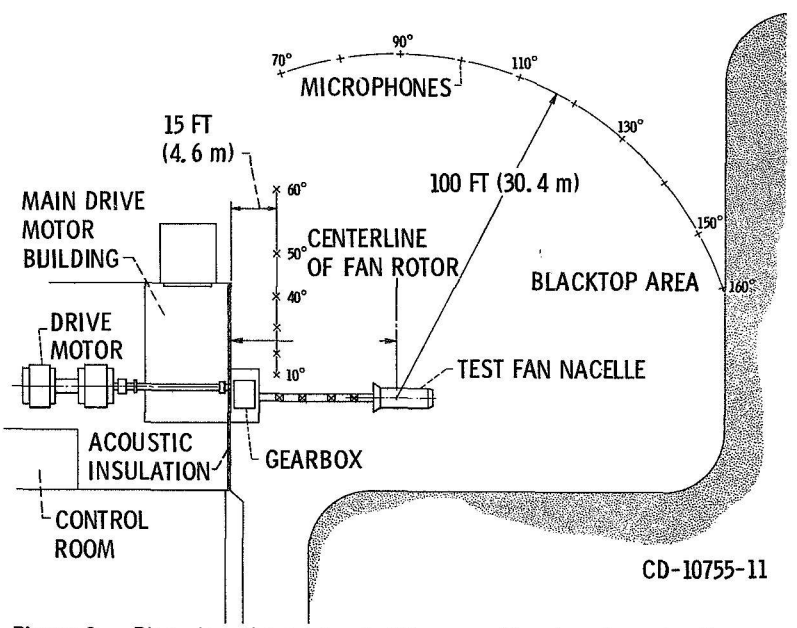

Figure 2. - Plan view of quiet fan facility area with microphone locations. Microphones at fan shaft elevation, (5.8 m) 19 feet above ground. (Scale: 1 cm = 2.4 m); 1 in. = 20 ft.

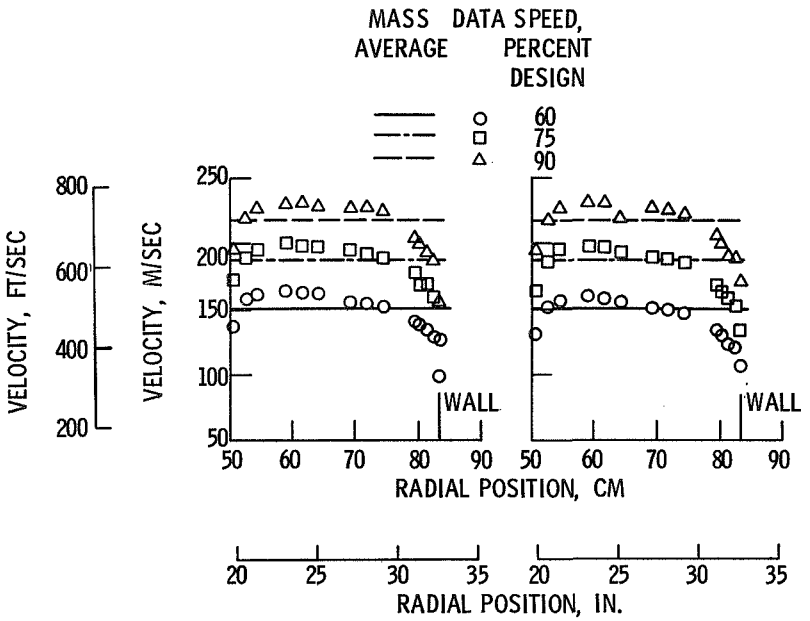

(A) HARD WALL, CONFIGURATION 1.

(B) LINED WALL, CONFIGURATION 13.

Figure 3. - Nozzle exit velocity profile.

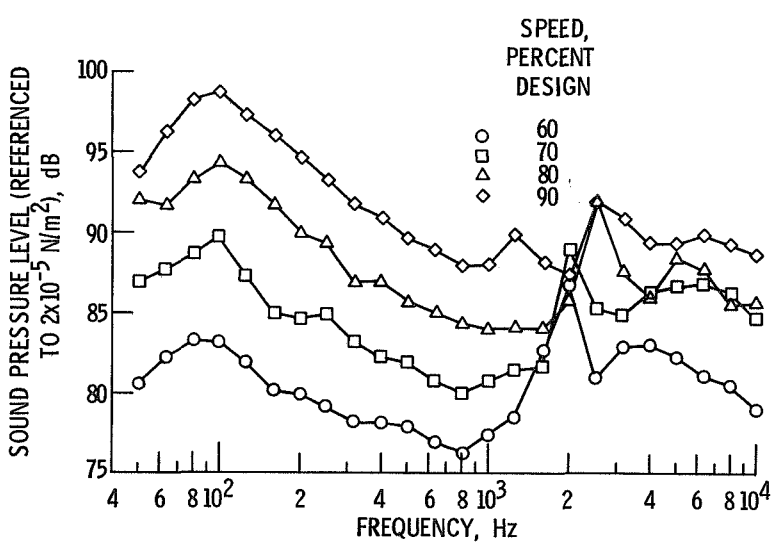

Figure 4. - Spectra of sound pressure level. Radius, 30.5 meters (100 ft) 160^0; Configuration 1: short inlet, 110-percent nozzle, hard wall.

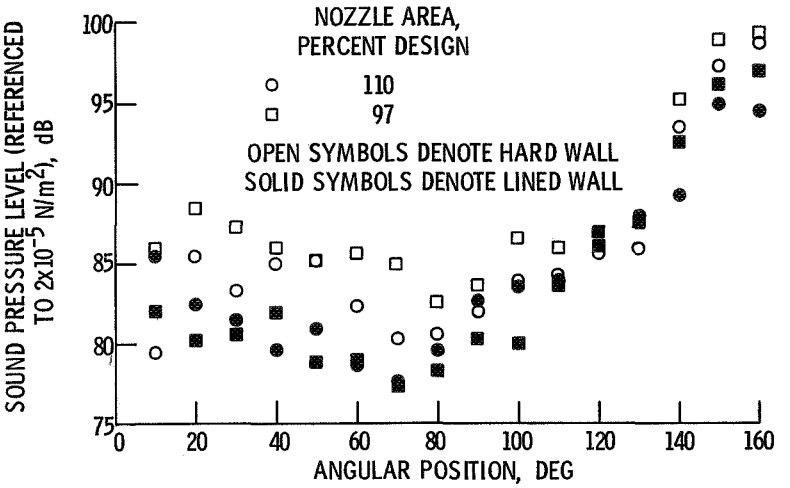

Figure 5. - Angular distribution of 1/3 octave sound pressure level for short-inlet configuration at 100 Hertz. Radius, 30.5 meters (100 ft); speed, 90 percent design.

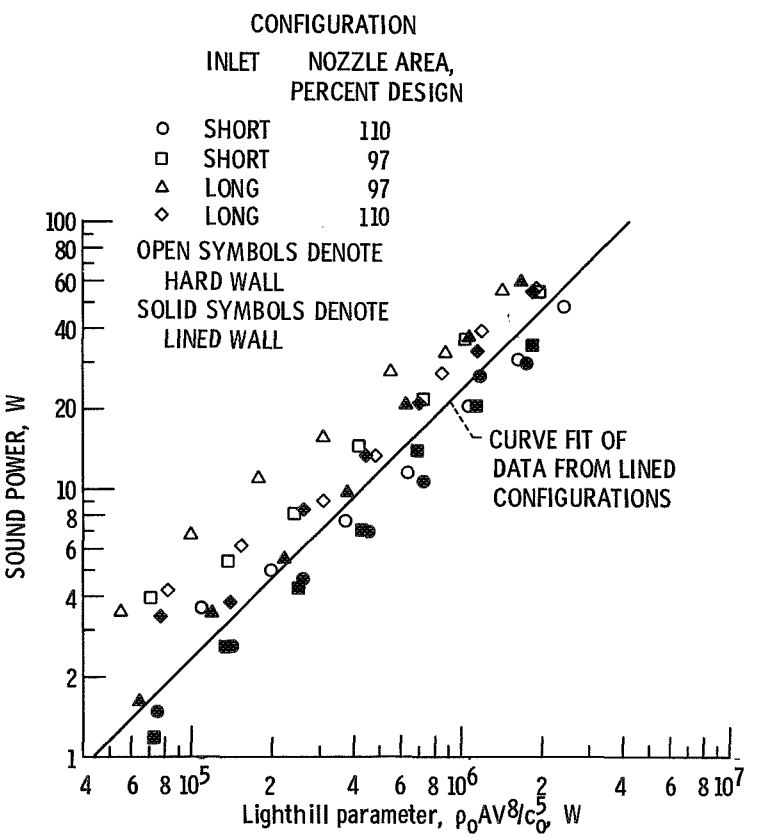

Figure 6. - Noise power as function of Lighthill parameter.

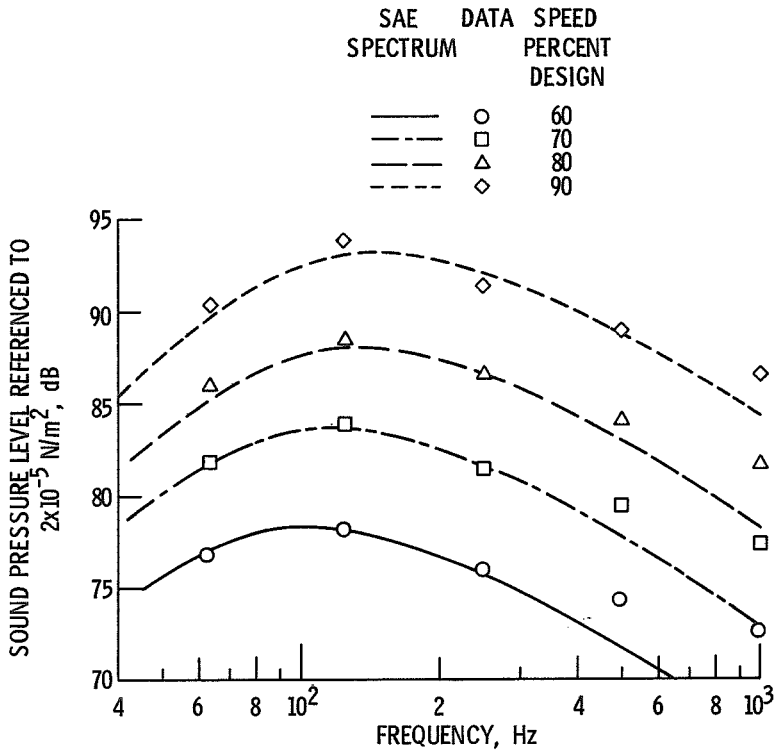

Figure 7. - Comparison between SAE standard spectrum and data of sound pressure level. Radius, 30.5 meters (100 feet), 150°; configuration 13: short inlet, 110 percent nozzle, lined wall.

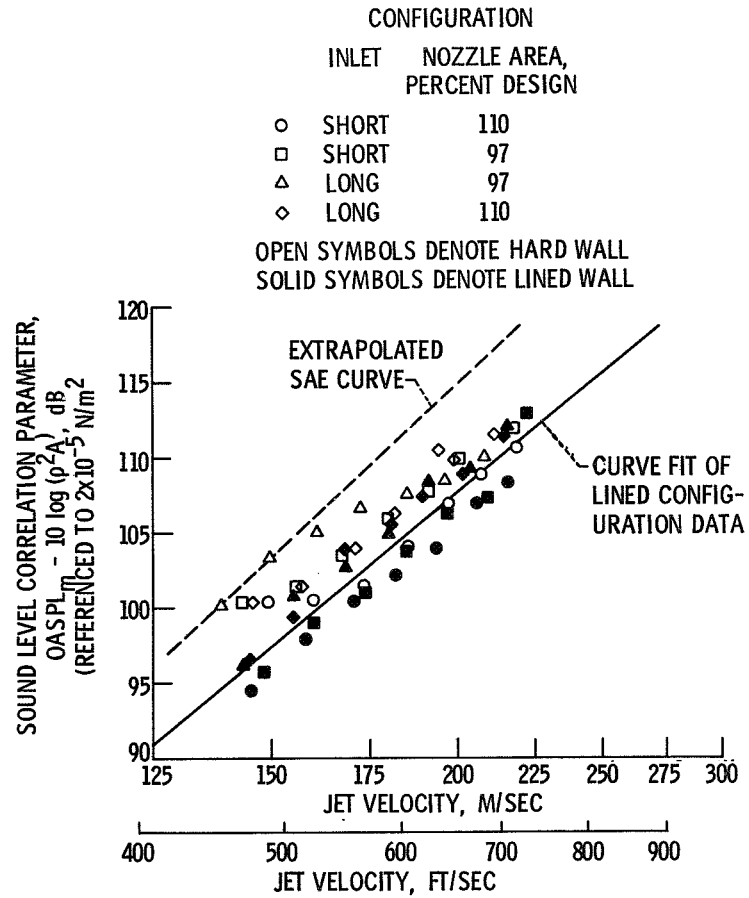

Figure 8. - Sound level as function of jet velocity. Sideline 30.5 meters (100 feet).

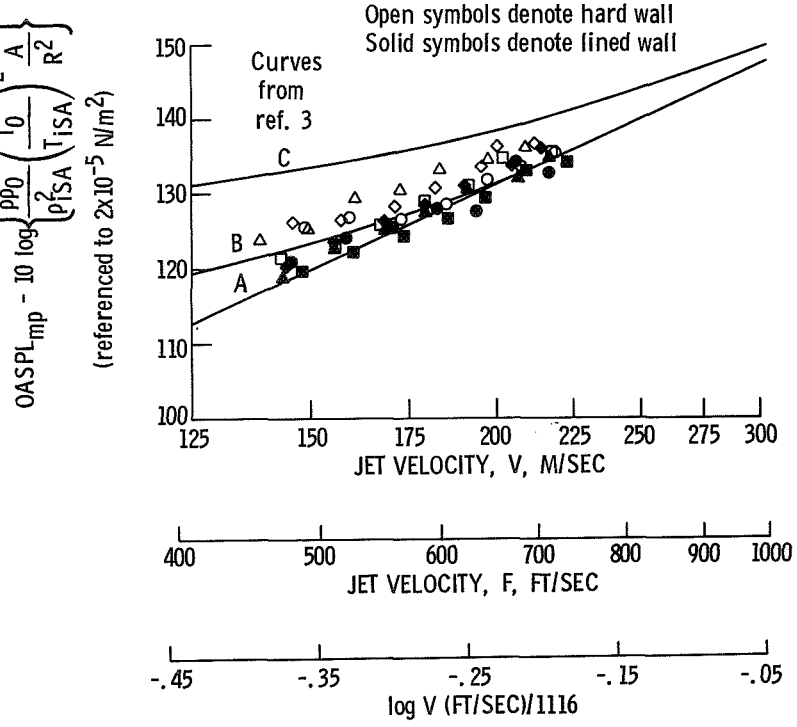

Figure 9. - Maximum polar sound level as function of jet velocity.

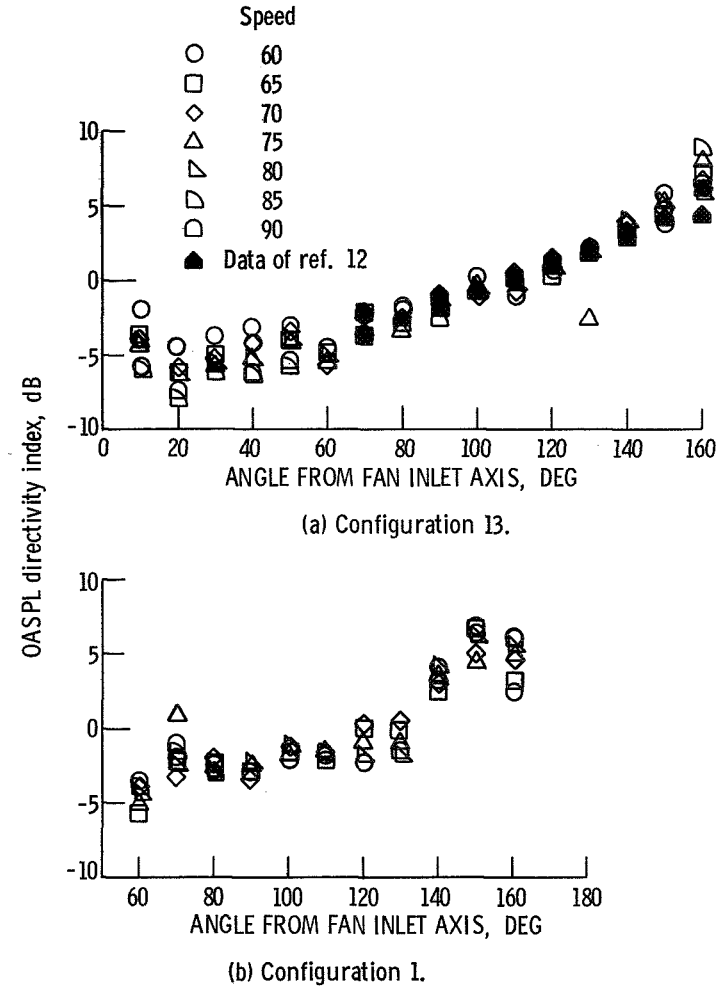

(a) Configuration 13.

(b) Configuration 1.

Figure 10. - Jet noise directivity index as a function of angle configuration: Short inlet, 110 percent nozzle, lined wall.

E-6124

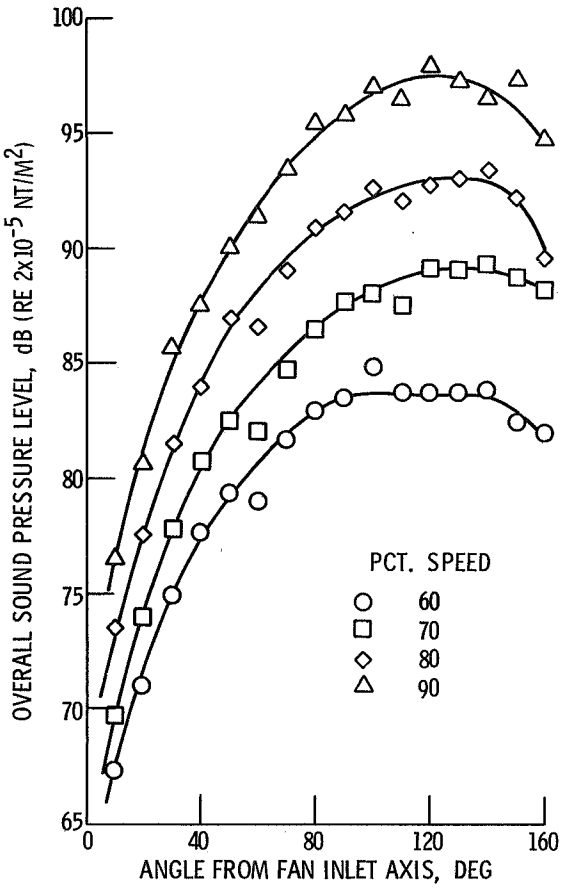

Figure 11. - Jet noise overall sound pressure level as a function of angle on a 30.5 m (100 ft) sideline. Configuration 13: Short inlet, 110 percent nozzle, lined wall.